Ab initio energetics and kinetics study of H$_2$ and CH$_4$ in the SI clathrate hydrate

Qi Li,[1] Brian Kolb,[1] Guillermo Román-Pérez,[2] José M. Soler,[2] Felix Yndurain,[2] Lingzhu Kong,[3] D. C. Langreth,[3] and T. Thonhauser[1,*]

[1]*Department of Physics, Wake Forest University, Winston-Salem, North Carolina 27109, USA*
[2]*Departamento de Física de la Materia Condensada, Universidad Autónoma de Madrid, Cantoblanco, E-28049 Madrid, Spain*
[3]*Department of Physics and Astronomy, Rutgers University, Piscataway, New Jersey 08854, USA*

We present *ab initio* results at the density functional theory level for the energetics and kinetics of H$_2$ and CH$_4$ in the SI clathrate hydrate. Our results complement a recent article by some of the authors [G. Román-Pérez *et al.*, Phys. Rev. Lett. **105**, 145901 (2010)] in that we show additional results of the energy landscape of H$_2$ and CH$_4$ in the various cages of the host material, as well as further results for energy barriers for all possible diffusion paths of H$_2$ and CH$_4$ through the water framework. We also report structural data of the low-pressure phase SI and the higher-pressure phases SII and SH.

Clathrate hydrates are crystalline, ice-like structures formed out of water molecules.[1] The water framework creates cavities in which gas molecules—typically O$_2$, H$_2$, CO$_2$, CH$_4$, Ar, Kr, Xe—can be trapped, which stabilize the framework. The existence of clathrates was first documented in 1810 by Sir Humphry Davy, and clathrates became the subject of intensive studies in the 1930s, when oil companies became aware that clathrates can block pipelines.[2] Nowadays, clathrate hydrates are of particular interest for two reasons: (i) they are formed naturally at the bottom of the ocean, where they are often filled with CH$_4$.[3] These deposits mean a tremendous stock pile of energy, while—at the same time—representing a possible global warming catastrophe if released uncontrolled into the environment through melting; (ii) clathrate hydrates can be used to store H$_2$ in its cavities and can be a viable hydrogen-storage material (albeit with moderate hydrogen-storage density).[4] For both cases, an understanding of the interaction between the guest molecule and the host framework is crucial for their formation and melting processes, which are still poorly understood.[5] In this brief report, we present results that elucidate this crucial guest-molecule/host-framework interaction and complement a recent paper by some of the authors.[6] We show additional results of the energy landscape of H$_2$ and CH$_4$ in the various cages of the host material, and we show further results for energy barriers for all possible diffusion paths of H$_2$ and CH$_4$ through the water framework. We also report structural data of the phases SI, SII, and SH.

At low pressure, the methane-filled clathrate forms the structure SI, consisting of two types of cages. The smaller cage is built of water molecules on the vertices of 12 pentagons with a diameter of approximately 7.86 Å,[7] and we refer to this as 5^{12} cage, or alternatively as D cage. The larger cage is built of 12 pentagons and 2 hexagons with a diameter of approximately 8.62 Å, and we call it $5^{12}6^2$ or T cage. The unitcell has cubic symmetry and consists of two 5^{12} and six $5^{12}6^2$ cages, with a total of 46 water molecules. At 250 MPa, the structure SI transforms into a new cubic phase SII, consisting of sixteen 5^{12} and eight $5^{12}6^4$ cages, containing 136 water molecules in its unitcell.[2] When the pressure is increased to 600 MPa, the structure undergoes another phase transition to the hexagonal

phase SH.[2] This phase has a smaller unitcell of three 5^{12}, two $4^3 5^6 6^3$, and one $5^{12}6^8$ cages, with only 34 water molecules. Very nice graphical representations of the different cages and structures can be found in Refs. 2, 4, 6, and 8. While other clathrate-hydrate structures exist, structure SI, SII, and SH are the most common ones.[2]

Guest molecules such as H$_2$ and CH$_4$ in the cavities of the clathrate hydrates interact with the water framework through van der Waals forces. But even the water framework itself, i.e., the interaction of water molecules through hydrogen bonds, has a van der Waals component.[9] To capture these effects, we perform here density functional theory (DFT) calculations utilizing the truly nonlocal vdW-DF functional, which includes van der Waals interactions seamlessly into DFT.[10–12] We implemented vdW-DF using a very efficient FFT formulation[13] into the latest release of PWSCF, which is a part of the QUANTUM-ESPRESSO package.[14] For our calculations we used ultrasoft pseudopotentials with a kinetic energy cutoff for wave functions and charge densities of 35 and 280 Ry, respectively. A self-consistency convergence criterion of at least 1×10^{-8} Ry was used. All structures were fully optimized with respect to volume and atom positions, and the force convergence threshold was at least 10^{-4} Ry/a.u. for SI and SH. We have also performed structural calculations on SII, but—due to the large unit cell with 136 water molecules, i.e., 408 atoms—we used a slightly less tight force convergence criterium of 5×10^{-4} Ry/a.u. For SI and SH we used a $2 \times 2 \times 2$ Monkhorst-Pack k-mesh,[15] while for SII we performed Γ-point calculations only.

The empty cages are experimentally not stable, but they have been shown to be a good starting point for calculations like ours.[6] We have calculated the optimized lattice parameters for the SI, SII, and SH structures and the results are collected in Table I. We have also calculated the structures when filled with methane (one methane molecule per cage) and filled with hydrogen (up to four H$_2$ per cage), but the lattice parameters expand less than 0.1% upon filling, such that we have used the parameters for the empty cages henceforth. Overall, our optimized lattice constants agree well with previous calculations[6] and experiment.[8] In Table I we further analyze the structure of the host materials by calculating the

TABLE I. Calculated and experimental lattice constants a and c for the SI, SII, and SH clathrate hydrates. In addition, calculated and experimental average nearest-neighbor and next-nearest-neighbor distances are given, as well as bond angles. Standard deviations are provided in square brackets. Experimental values for the lattice constants are taken from Ref. 8 for methane-filled cages. Experimental values for the averaged quantities are calculated from the structures given in the supplemental materials of Ref. 8. The experimental distances d_{O-H}^{nn} (d_{O-H}^{nnn}) seem to be underestimated (overestimated), most likely due to the difficulty of accurately determining H positions in x-ray experiments. For SI, neutron scattering experiments suggest $d_{O-H}^{nn} = 0.97$ Å and $d_{O-O}^{nn} = 2.755$ Å.[16] Also note that there is some variation in the experimental results for the lattice constants in Refs. 1, 4, and 8.

		a [Å]	c [Å]	d_{O-H}^{nn} [Å]	d_{O-H}^{nnn} [Å]	d_{O-O}^{nn} [Å]	$\angle_{H-O-H}$[°]	$\angle_{O-O-O}$[°]
SI	Calc.	11.97	–	0.994 [0.001]	1.790 [0.014]	2.781 [0.013]	107.1° [1.0]	108.6° [4.0]
	Exp.	11.88	–	0.861 [0.031]	1.911 [0.022]	2.761 [0.017]	109.3° [3.0]	108.7° [3.7]
SII	Calc.	17.35	–	0.994 [0.001]	1.792 [0.016]	2.784 [0.016]	107.1° [0.6]	109.2° [4.3]
	Exp.	17.19	–	0.812 [0.016]	1.959 [0.025]	2.768 [0.013]	109.5° [2.0]	109.3° [4.0]
SH	Calc.	12.32	10.01	0.994 [0.001]	1.793 [0.015]	2.782 [0.011]	107.2° [0.9]	108.4° [8.5]
	Exp.	12.33	9.92	0.781 [0.040]	1.955 [0.022]	2.775 [0.005]	108.9° [5.1]	108.4° [8.3]

average nearest-neighbor and next-nearest-neighbor distances and important bond angles. In general, the calculated average distances and angles vary only insignificantly among SI, SII, and SH, whereas they show a slightly larger spread for some experimental values. As a side-note, for a single water molecule we calculate $d_{O-H} = 0.973$ Å and $\angle_{H-O-H} = 104.9°$, in good agreement with the experimental numbers of 0.958 Å and 104.5°.[17] Note that vdW-DF is known to give slightly too large binding distances.[18,19] Small deviations are visible in the distances d_{O-H}^{nn} and d_{O-H}^{nnn}, which in sum mostly cancel to give very good agreement with the experimental O–O distances. Reference 8 also gives the O–O distances for all structures explicitly as between 2.725 and 2.791 Å, in remarkable agreement with our calculations. Also, our calculated angles $\angle_{O-O-O}$ agree very well with experiment. However, the good agreement between oxygen distances and angles—which describe the structure as a whole—is closely related to the agreement for the lattice constants.

We next focus on the binding energies of guest molecules in the SI structure. In particular, we study the binding energies of CH_4 and H_2 in the D and T cages as a function of the number of molecules; results are depicted in Fig. 1 for calculations where molecules are added to only one cage in the unitcell, while all other cages are kept empty. Here, we
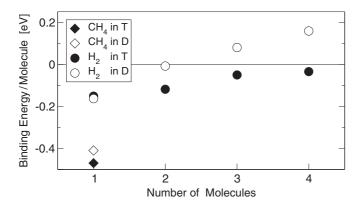
define the binding energy as the energy difference between the "water-framework + guest-molecules" system minus the energy of the single constituents. In case of n-fold occupied cages, we subtract n times the energy of the single molecule. Methane is a large molecule compared to the cage sizes and it can be seen that in both D and T only one methane molecule can be stored. Upon adding another methane molecule, the binding energy increases drastically. The situation is different for the much smaller H_2 molecules. In the smaller D cage we can store up to two H_2 molecules, but increasing the number to three or four results in a positive binding energy; i.e., work is required to place more than two molecules into this cage. Note that the binding energy that we find for double H_2 occupancy is rather small, i.e., -8 meV/per molecule. It is, thus, likely that at nonzero temperatures cages are only singly occupied. Experimentally, while the majority of recent work seems to favor single occupancy of the D cages (see, e.g., Ref. 20), there are also reports that propose double occupancy or that find inconclusive evidence.[21–25] On the other hand, the larger T cage can store four H_2 molecules. If a fifth molecule is added, it escapes through one of the hexagonal faces into the neighboring, empty T cage. Our calculated H_2 storage capacity of four molecules in the T cages is in agreement with experiment.[4] The binding energy for one H_2 molecule compares well with quantum-chemistry calculations on isolated cavities, which give -0.123 eV.[21] Overall, our binding energies are slightly smaller than the ones in Ref. 6. Note that quantum motions have been neglected in our approach, which may play an important role in the binding process and when determining the cage occupancy. A more precise treatment requires the computation of the corresponding thermodynamic partition function, as, for example, shown in Ref. 26. Nevertheless, we consider our calculations for the binding energy an important first step that already reveals important information.

It is also interesting to study where and how the H_2 and CH_4 molecules bind in the cages. If only one molecule is present in the cages, it binds in the center of the cage. Rotations and small displacements of H_2 in that situation are on an energy scale of approximately 1 meV and approach the accuracy of our calculations. At room temperature, such
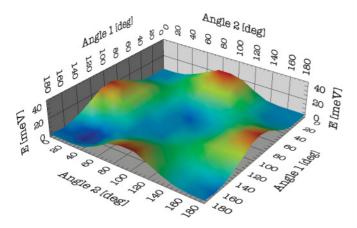

FIG. 1. Binding energies per molecule for different numbers of CH_4 and H_2 molecules in the D and T cages of SI. While the D and T cages can store only one CH_4 molecule, the D and T cage can store up to two and four H_2 molecules, respectively.

FIG. 2. (Color online) Energy landscape in meV for a rotating methane molecule in a D cage. The x and y axes correspond to rotations about two mutually perpendicular axes. At the (0,0) point of the plot, the hydrogen atoms of the methane point exactly toward four oxygens of the D cage. The difference between the minimum and maximum energy is 22 meV.
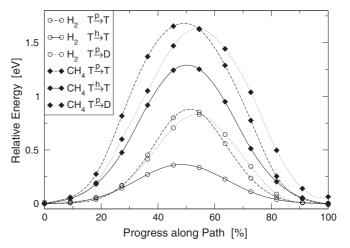

FIG. 3. Barriers to diffusion of H_2 and CH_4 through the water framework along different paths, as a function of the relative progress along the path. The plots are labeled as $A \xrightarrow{x} B$, where A is the type of the starting cage, B is the type of the ending cage, and x refers to either pentagon (p) or hexagon (h), indicating the opening being used for traversing. The symbols are the results from 12-image NEB calculations and the lines are fitted cubic splines, serving as a guide to the eye.

perturbations are thus easily thermally activated. Since the methane molecule is larger, it cannot move/rotate as easily. We have studied the rotation of a single methane molecule centered in the D and T cages as a function of rotation about two mutually perpendicular axes. The energy landscape for this rotation is depicted in Fig. 2 for the D cage. The D cage with its 12 pentagons and the methane molecule have a related symmetry, which allows us to choose the (0,0) point of the plot such that all methane hydrogens point exactly to an oxygen of the host lattice. At this point, hydrogen bonds are created and the total energy is the lowest. Upon rotation of the methane, the hydrogen bonds break and the energy increases. The difference between the lowest and highest point of this energy landscape is 22 meV, suggesting thermal activation of rotations at room temperature and quantifying an experimental assumption.[8] We have also studied the rotation of a methane molecule in a T cage and the results are very similar to the results presented in Fig. 2, with the difference that the maximal energy barrier is slightly smaller, i.e., 18 meV, which is not surprising, as the T cage is slightly larger and the methane molecule can rotate more easily. Calculations for both rotation-energy landscapes have independently also been performed using SIESTA[27,28] and give essentially identical results.

Finally, we present results for barriers to diffusion through the water framework in the SI structure. In the case of H_2 and hydrogen storage this is of much interest, as practical storage solutions require fast kinetics, i.e., low barriers. In the case of CH_4, the barriers can help us understand the natural formation of the filled clathrates. We have calculated the barriers to diffusion with nudged elastic band (NEB) calculations, using 12 images along the path from the center of one cage to the center of the next cage; the results for all possible paths are plotted in Fig. 3. Note that the relaxation of the host lattice is crucial to obtain accurate barrier energies,[6] and NEB calculations allow for such relaxations perpendicular to the path automatically. The plots are labeled as $A \xrightarrow{x} B$, where A is the type of the starting cage, B is the type of the ending

cage, and x refers to either pentagon (p) or hexagon (h), indicating the opening being used for traversing. Note that for the path $T \xrightarrow{p} D$ there is only one choice of opening, i.e., a pentagon, and the path is not symmetric as the distance from the center of T to its edge is longer than the corresponding distance in the D cage. Furthermore, this path's end energy is different from its starting energy, since the guest molecules are binding with different binding energies in the cages T and D, as already evident from Fig. 1. The lowest barriers for H_2 and CH_4 diffusion agree well with previous calculations.[6,29] But, our H_2 diffusion barrier is an overestimation with respect to a recent NMR experiment, which gives 0.03 eV and warrants further investigation.[30] The barriers are in general smaller for diffusion through hexagons, simply because these openings are larger.

For hydrogen-storage applications, the low barrier of ~0.3 eV between T cages (going through a hexagon) is important. Through these T-cage channels, which thread through the material in all three dimensions, the hydrogen can quickly be absorbed or released. However, to achieve the material's full storage potential, some hydrogen molecules will also have to get into the D cages, with a much higher barrier of ~0.75 eV. The large barrier of ~1.4 eV for methane diffusion suggests that the methane molecules get trapped while the clathrate is formed, rather than diffusing into an already existing empty clathrate.

To conclude, we have performed an *ab initio* study of structural, energetic, and kinetic properties of the guest molecules H_2 and CH_4 in hydrate clathrates. We have also shown first results for the difficult-to-model, high-pressure phase SII with a large unit cell, finding good agreement with experiment. While we have used vdW-DF for our study, it is conceivable that its successor, vdW-DF2,[19] may further

improve upon our results. We encourage additional studies of the hydrate clathrates using vdW-DF2, also including other types of cages, and more detailed studies of the SII phase, which is one of the more promising phases among the hydrate clathrates for hydrogen-storage applications.

*thonhauser@wfu.edu

[1] E. D. Sloan and C. A. Koh, *Clathrate Hydrates* (CRC, Boca Raton, 2008).

[2] W. L. Mao, C. A. Koh, and E. D. Sloan, Phys. Today **60**, 42 (2007).

[3] B. Buffett and D. Archer, Earth Planet. Sci. Lett. **227**, 185 (2004).

[4] V. V. Struzhkin, B. Militzer, W. L. Mao, H.-k. Mao, and R. J. Hemley, Chem. Rev. **107**, 4133 (2007).

[5] S. Gao, W. House, and W. G. Chapman, J. Phys. Chem. B **109**, 19090 (2005).

[6] G. Román-Pérez, M. Moaied, J. M. Soler, and F. Yndurain, Phys. Rev. Lett. **105**, 145901 (2010).

[7] Here, we define the diameter as twice the average distance between oxygen atoms and the cage center.

[8] M. T. Kirchner, R. Boese, W. E. Billups, and L. R. Norman, J. Am. Chem. Soc. **126**, 9407 (2004).

[9] B. Kolb and T. Thonhauser, Phys. Rev. B **84**, 045116 (2011).

[10] M. Dion, H. Rydberg, E. Schröder, D. C. Langreth, and B. I. Lundqvist, Phys. Rev. Lett. **92**, 246401 (2004); **95**, 109902(E) (2005).

[11] T. Thonhauser, V. R. Cooper, S. Li, A. Puzder, P. Hyldgaard, and D. C. Langreth, Phys. Rev. B **76**, 125112 (2007).

[12] D. C. Langreth *et al.*, J. Phys. Condens. Mattter **21**, 084203 (2009).

[13] G. Román-Pérez and J. M. Soler, Phys. Rev. Lett. **103**, 096102 (2009).

[14] P. Giannozzi *et al.*, J. Phys. Condens. Matter **21**, 395502 (2009).

[15] H. J. Monkhorst and J. D. Pack, Phys. Rev. B **13**, 5188 (1976); J. D. Pack and H. J. Monkhorst, *ibid*. **16**, 1748 (1977).

[16] C. Gutt, B. Asmussen, W. Press, M. R. Johnson, Y. P. Handa, and J. S. Tse, J. Chem. Phys. **113**, 4713 (2000).

[17] G. Graner, E. Hirota, T. Iijima, K. Kuchitsu, D. A. Ramsay, J. Vogt, and N. Vogt, *2 Inorganic Molecules. Part 4*, K. Kuchitsu, (ed.), SpringerMaterials—The Landolt-Börnstein Database [http://www.springermaterials.com]. DOI: 10.1007/10529543_6.

[18] T. Thonhauser, A. Puzder, and D. C. Langreth, J. Chem. Phys. **124**, 164106 (2006).

[19] K. Lee, E. D. Murray, L. Kong, B. I. Lundqvist, and D. C. Langreth, Phys. Rev. B **82**, 081101(R) (2010).

[20] K. A. Lokshin, Y. Zhao, D. He, W. L. Mao, H.-K. Mao, R. J. Hemley, M. V. Lobanov, and M. Greenblatt, Phys. Rev. Lett. **93**, 125503 (2004).

[21] S. Patchkovskii and J. S. Tse, Proc. Nat. Acad. Sci. USA **100**, 14645 (2003).

[22] T. M. Inerbaev, V. R. Belosludov, R. V. Belosludov, M. Sluiter, and Y. Kawazoe, Comput. Mater. Sci. **36**, 229 (2006).

[23] F. Sebastianelli, M. Z. Xu, Y. S. Elmatad, J. W. Moskowitz, and Z. Bacic, J. Phys. Chem. C **111**, 2497 (2007).

[24] L. J. Florusse, C. J. Peters, J. Schoonman, K. C. Hester, C. A. Koh, S. F. Dec, K. N. Marsh, and E. D. Sloan, Science **306**, 469 (2004).

[25] J. Wang, H. Lu, J. A. Ripmeester, and U. Becker, J. Phys. Chem. C **114**, 21042 (2010).

[26] S. Patchkovskii and S. N. Yurchenko, PhysChemChemPhys **6**, 4152 (2004).

[27] J. M. Soler, E. Artacho, J. D. Gale, A. Garcia, J. Junquera, P. Ordejón, and D. Sánchez-Portal, J. Phys. Condens. Matter **14**, 2745 (2002).

[28] P. Ordejón, E. Artacho, and J. M. Soler, Phys. Rev. B **53**, R10441 (1996).

[29] S. Alavi and J. A. Ripmeester, Angew. Chem. **119**, 6214 (2007).

[30] T. Okuchi, I. L. Moudrakovski, and J. A. Ripmeester, Appl. Phys. Lett. **91**, 171903 (2007).